NUMERICAL SIMULATION OF COMBUSTION IN INERT POROUS MEDIA

Roberto Carlos Moro Filho
Marcelo J S de Lemos
Departamento de Energia - IEME
Instituto Tecnológico de Aeronáutica – ITA
12228-900 – São José dos Campos – SP - Brasil
rmoro@.ita.br
delemos@mec.ita.br

Abstract. *This paper presents numerical methods for the simulation of combustion processes in porous media using a 1-step global mechanism. The model is based on a macroscopic formulation of the heat and mass transport equations for laminar and turbulent flow. The concept of the double-decomposition, which considers both time fluctuations and spatial deviations about mean values is used. The effects of the model on temperature, and species are examined.*

Keywords: *porous media burner, premixed flame, numerical simulation.*

1. INTRODUCTION

According to Pantangi et al. (2006), porous media combustion devices can be classified into two categories, one in which the combustion is fully confined within the pores of the porous structure and the other one in which the combustion takes place over the surface of the porous matrix. The first one is receiving more attention of researchers due to the numerous advantages, burning of lean combustible mixtures, higher ranges of flame stability, lower pollutant formation, etc. (Howell et al. (1996)). Systems based on fluidized bed combustion, in-situ combustion for oil recovery, household heating combustion, are just a few examples of such applications (Trimis and Durst (1996)).

In most of the studies of premixed combustion within inert porous media the flow is assumed to be laminar and one-dimensional, the change in the pressure across the flame is generally negligible compared to the absolute pressure, and the pressure is assumed constant (Baek (1989),Yoshizawa et al. (1988),Hsu et al. (1993),Neef et al. (1999)). The use of single-step global chemistry (Mohamad et al. (1994)) is common. The inadequacies of global kinetics are well recognized, Hsu et al. (1993) presents a comparison between one-step and multi-step chemistry.

Turbulence modeling of combustion within inert porous media has been conducted by Lim and Matthews (1993)on the basis of an extension of the standard k - ε model of Jones and Launder (1972). Work on direct simulation of turbulence in premixed flames, for the case when the porous dimension is of the order of the flame thickness, has also been reported in Sahraoui and Kaviany (1995).

Studies on macroscopic transport modeling of incompressible flows in porous media have been based on the volume-average methodology for either heat or mass transfer. In turbulent flows, when time fluctuations of the flow properties are also considered in addition to spatial deviations, there are two possible methodologies to follow in order to obtain macroscopic equations, one, can be the application of time-average operator followed by volume-averaging, and, the other, the application of volume-averaging before time-averaging is applied. However, both sets of macroscopic transport equations are equivalent when examined under the recently established double decomposition concept (Pedras and de Lemos (2000),Pedras and de Lemos (2001a),Pedras and de Lemos (2001b),Pedras and de Lemos (2001c)). The works of Pedras and de Lemos have been extended to heat and mass transfer in porous media where both time fluctuations and spatial deviations were considered for temperature(Pedras et al. (2003)) and mass fraction(De-Lemos e Mesquita (2003)).

Because of important influence of lateral heat loss in porous medium burners, a two dimensional model is necessary. The present paper follows the foregoing works and presents a two dimensional mathematical model for laminar and turbulent pre-mixed flame combustion in porous media although in this first work only computations of a one-dimensional laminar pre-mixed flame of methane/air is presented. The numerical methodology employed is based on the control-volume approach with a boundary-fitted non-orthogonal coordinate system. The reactor consists of a two-region burner with a small pore size upstream and a large pore size downstream in order to achieve steady combustion in the porous media, the flame can be stabilized at the interface between the two different porosity blocks. The effects of thermal power and excess air ratio are discussed. Radiation, dispersion, thermal nonequilibrium, and turbulence, are subjects of ongoing investigations and will be addressed in subsequent papers.

2. MACROSCOPIC TRANSPORT EQUATIONS

Macroscopic transport equations for turbulent flow in a porous medium are obtained through the simultaneous application of time and volume average operators over a generic fluid property φ (see Pedras and de Lemos (2000),Pedras and de Lemos (2001a),Pedras and de Lemos (2001b),Pedras and de Lemos (2001c),Pedras and de Lemos (2003)).

2.1 Macroscopic continuity equation

$$\nabla.\mathbf{u}_D = 0 \tag{1}$$

where, $\mathbf{u}_D$ is the average surface velocity (also known as seepage, superficial, filter or Darcy velocity). Equation (1) represents the macroscopic continuity equation for an incompressible fluid.

2.2 Macroscopic momentum equation

$$\rho\left[\nabla\cdot\left(\frac{\overline{\mathbf{u}}_D\,\overline{\mathbf{u}}_D}{\phi}\right)\right] = -\nabla(\phi\langle\overline{p}\rangle^i) + \mu\nabla^2\overline{\mathbf{u}}_D - \nabla\cdot(\rho\phi\langle\overline{\mathbf{u}'\mathbf{u}'}\rangle^i) - \left[\frac{\mu\phi}{K}\overline{\mathbf{u}}_D + \frac{c_F\phi\rho|\overline{\mathbf{u}}_D|\,\overline{\mathbf{u}}_D}{\sqrt{K}}\right] \tag{2}$$

where the last two terms in equation (2), represent the Darcy-Forchheimer contribution. The symbol K is the porous medium permeability, $c_F = 0.55$ is the form drag coefficient (Forchheimer coefficient), $\langle p\rangle^i$ is the intrinsic (volume-averaged on fluid phase) pressure of the fluid, ρ is the fluid density and is a function of temperature, μ represents the fluid dynamic viscosity and ϕ is the porosity of the porous medium.

The turbulence is modeled using a macroscopic $k-\varepsilon$ model given by,

$$\rho\left[\nabla\cdot\left(\overline{\mathbf{u}}_D\langle k\rangle^i\right)\right] = \nabla\cdot\left[\left(\mu+\frac{\mu_{t_\phi}}{\sigma_k}\right)\nabla\left(\phi\langle k\rangle^i\right)\right] - \rho\langle\overline{\mathbf{u}'\mathbf{u}'}\rangle^i:\nabla\overline{\mathbf{u}}_D + c_k\rho\frac{\phi\langle k\rangle^i|\overline{\mathbf{u}}_D|}{\sqrt{K}} - \rho\phi\langle\varepsilon\rangle^i \tag{3}$$

$$\rho\left[\nabla\cdot\left(\overline{\mathbf{u}}_D\langle\varepsilon\rangle^i\right)\right] = \nabla\cdot\left[\left(\mu+\frac{\mu_{t_\phi}}{\sigma_\varepsilon}\right)\nabla\left(\phi\langle\varepsilon\rangle^i\right)\right] + c_1\left(-\rho\langle\overline{\mathbf{u}'\mathbf{u}'}\rangle^i:\nabla\overline{\mathbf{u}}_D\right)\frac{\langle\varepsilon\rangle^i}{\langle k\rangle^i} + c_2\,c_k\,\rho\frac{\phi\langle\varepsilon\rangle^i|\overline{\mathbf{u}}_D|}{\sqrt{K}} - c_2\,\rho\phi\frac{\langle\varepsilon\rangle^{i\,2}}{\langle k\rangle^i} \tag{4}$$

where,

$$\mu_{t_\phi} = \rho c_\mu\frac{\langle k\rangle^{i\,2}}{\langle\varepsilon\rangle^i} \tag{5}$$

and,

$$-\rho\phi\langle\overline{\mathbf{u}'\mathbf{u}'}\rangle^i = \mu_{t_\phi}\,2\langle\overline{\mathbf{D}}\rangle^{\mathbf{v}} - \frac{2}{3}\phi\rho\langle k\rangle^i\mathbf{I} \tag{6}$$

is the macroscopic Reynolds tensor which is modeled in analogy with Boussinesq hypothesis and its generalized form proposed by Kolmogorov (1942).

2.3 Macroscopic Energy Equation

$$\left(\rho\,c_p\right)_f\,\nabla\cdot\left(\mathbf{u}_D\langle\overline{T}\rangle^i\right) = \nabla\cdot\left\{\mathbf{K}_{eff,f}\cdot\nabla\langle\overline{T}\rangle^i\right\} + \phi\Delta HS_{fu} \tag{7}$$

where, $\langle\overline{T}\rangle^i$ is the averaged temperature for both the solid and the liquid according to the concept of local thermal equilibrium Kaviany (1995), ΔH is the heat of combustion, S_{fu} is the rate of fuel consumption determined by a one-step Arrehnious rate equation, to be shown below, K_{eff} is the effective conductivity tensor given by,

$$\mathbf{K}_{eff} = \left\{ \phi k_f + (1-\phi) \left[k_s + \frac{16\sigma \left(\langle \overline{T} \rangle^i \right)^3}{3\beta} \right] \right\} \mathbf{I} + \underbrace{\mathbf{K}_{tor}}_{tortuosity} + \underbrace{\mathbf{K}_{disp}}_{dispersion} + \underbrace{\mathbf{K}_{\mathrm{disp,t}} + \mathbf{K}_{\mathrm{t}}}_{turbulence} \tag{8}$$

where, k_f and k_s are the thermal conductivities for the fluid and for the solid, β is the extinction coefficient, σ is the Stefan-Boltzmann constant.

2.4 Macroscopic Mass Transport Equation

$$\nabla \cdot (\mathbf{u}_D \langle \overline{m_{fu}} \rangle^i) = \nabla \cdot \mathbf{D}_{eff} \cdot \nabla (\phi \langle \overline{m_{fu}} \rangle^i) + \phi S_{fu} \tag{9}$$

where m_{fu} is the local mass fraction for the fuel. The effective dispersion tensor, $\mathbf{D}_{eff}$, is defined as:

$$\mathbf{D}_{eff} = \mathbf{D}_{disp} + \mathbf{D}_{diff} + \mathbf{D}_t + \mathbf{D}_{disp,t} = \mathbf{D}_{disp} + \frac{1}{\rho} \left(\frac{\mu_\phi}{Sc_\ell} + \frac{\mu_{t_\phi}}{Sc_{\ell,t}} \right) \mathbf{I} = \mathbf{D}_{disp} + \frac{1}{\rho} \left(\frac{\mu_{\phi,ef}}{Sc_{\ell,ef}} \right) \mathbf{I} \tag{10}$$

where $\mathbf{D}_{disp}$ is the dispersion tensor and,

$$\mathbf{D}_t + \mathbf{D}_{disp,t} = \frac{1}{\rho} \frac{\mu_{t_\phi}}{Sc_{\ell,t}} \mathbf{I} \tag{11}$$

$$\mathbf{D}_{diff} = \langle D \rangle^i \mathbf{I} = \frac{1}{\rho} \frac{\mu_\phi}{Sc} \mathbf{I} \tag{12}$$

2.5 Combustion model

Premixed fuel and air enter the system which is characterized by two regions having different porosities. The region at the upstream end has a lower porosity than the one at the downstream end which works as a combustion chamber. The combustion reaction is assumed to occur in a single step according to the chemical equation

$$CH_4 + 2(1+\Psi)(O_2 + 3.76N_2) \longrightarrow CO_2 + 2H_2O + 2\Psi O_2 + 7.52(1+\Psi)N_2 \tag{13}$$

where, ψ is the excess air in the reactant stream at the inlet of porous foam and is related to the equivalent ratio Φ by,

$$\Psi = \frac{1}{\Phi} - 1 \tag{14}$$

where,

$$\Phi = \frac{(m_{fu} / m_{ox})}{(m_{fu} / m_{ox})_{st}} \tag{15}$$

The ratio of fuel consumption is given by,

$$S_{fu} = \rho^2 A \langle \overline{m_{fu}} \rangle^i \langle \overline{m_{Ox}} \rangle^i \exp[-E_a / R \langle \overline{T} \rangle^i] \tag{16}$$

where, A is the pre-exponential factor, E_a is the activation energy and R is the universal gas constant. The gas density is updated using the ideal gas equation in the form,

$$\rho = P_0 / R^* \langle \overline{T} \rangle^i \tag{17}$$

where, P_0 is a reference pressure, which is kept constant during the relaxation process, and $R^* = R / M$ and M is the gas molecular mass.

3. NUMERICAL MODEL

The governing equations were discretized using the finite volume procedure Patankar (1980) with a boundary-fitted non-orthogonal coordinate system. The SIMPLE algorithm for the pressure-velocity coupling was adopted to correct both the pressure and the velocity fields. The process starts with the solution of the two momentum equations. Then the velocity field is adjusted in order to satisfy the continuity principle. This adjustment is obtained by solving the pressure correction equation. After that, the turbulence model equations and the energy equation are relaxed to update the k, ε and mass fraction fields. Details on the numerical discretization can be found in de Lemos and Pedras (2001). A computational grid of 266x30 nodes are used in x- and y-direction.

4. RESULTS AND DISCUSION

4.1 Geometry and coordinate system

Figure 1 presents the geometry of the porous media burner consisting of two distinct regions with different porosities and permeability. The gas mixture enters at the inflow boundary at the left, and the combustion products leave the burner at the outflow boundary at the right. The walls are impermeable and isolated. The porosity ϕ_1 is smaller than ϕ_2. All numerical parameters are found in Table 1, the activation energy and the pre-exponential factor were obtained from Mohamad et al. (1994).

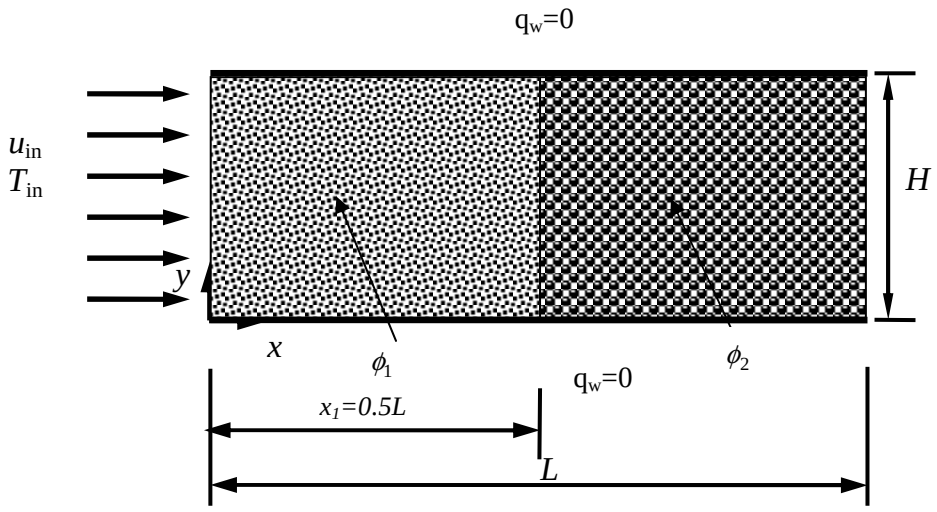

Figure 1. Geometry of a porous inert media burner and coordinate system.

4.2 Boundary conditions

The following boundary conditions are imposed on the solution:

$$\text{at x=0, } u = u_{in}\text{ , } v=0,\ \langle \overline{T} \rangle^{i} = T_{in},\ \langle \overline{m_{fu}} \rangle^{i} = m_{fu,in}, \tag{18}$$

$$\text{at x=L, } \frac{\partial \langle \overline{T} \rangle^{i}}{\partial x} = \frac{\partial \langle \overline{m_{fu}} \rangle^{i}}{\partial x} = \frac{\partial u}{\partial x} = \frac{\partial v}{\partial x} = 0 \tag{19}$$

where, u and v are the components of Darcy velocity vector in x and y. The non-slip condition for velocity is applied on both walls.

4.3 Temperature, concentration, and volumetric rate of fuel consumption profiles

Figure 2 presents the temperature, mass fraction of fuel, and volumetric rate of fuel consumption profiles for a rectangular adiabatic burner with an inlet velocity of 0.40 m/s, an excess air ratio of 0.67, and an inlet temperature of 335 K. The values for the one dimensional plots were taken at the center line of the combustor.

The profiles indicate that the effect of the porous matrix on the flame structure is the increase of the flame thickness due to the high conductibility of the solid phase.

Table 1. Operating Conditions

Quantity	Value
Activation energy (J/mol) - E_a	130×10^3
K_1 (m^2)	3.827×10^{-10}
K_2 (m^2)	9.375×10^{-9}
ϕ_1	0.3
ϕ_2	0.6
Pre-exponential factor in reaction rate – A (m^3/kg.s)	3.0×10^8
Length of the combustor – L (cm)	8
H (cm)	4
R (kJ/kmol.K)	8.3145
R^* (kJ/kgK)	0.301
P^0 (kN/m^2)	101.325
$m_{fuel,in}$	0.033784
T_{in} (K)	335

Figure 3 presents the pressure drop at the center line of the combustor where,

$$PN = \frac{P - P_{MIN}}{P_{MAX} - P_{MIN}} \tag{20}$$

The inflexion point at the abscissa x/L=0,5 represents the interface between the two porous materials. It was observed with additional simulations that the combustion affect the pressure drop slightly when compared with the flow without combustion.

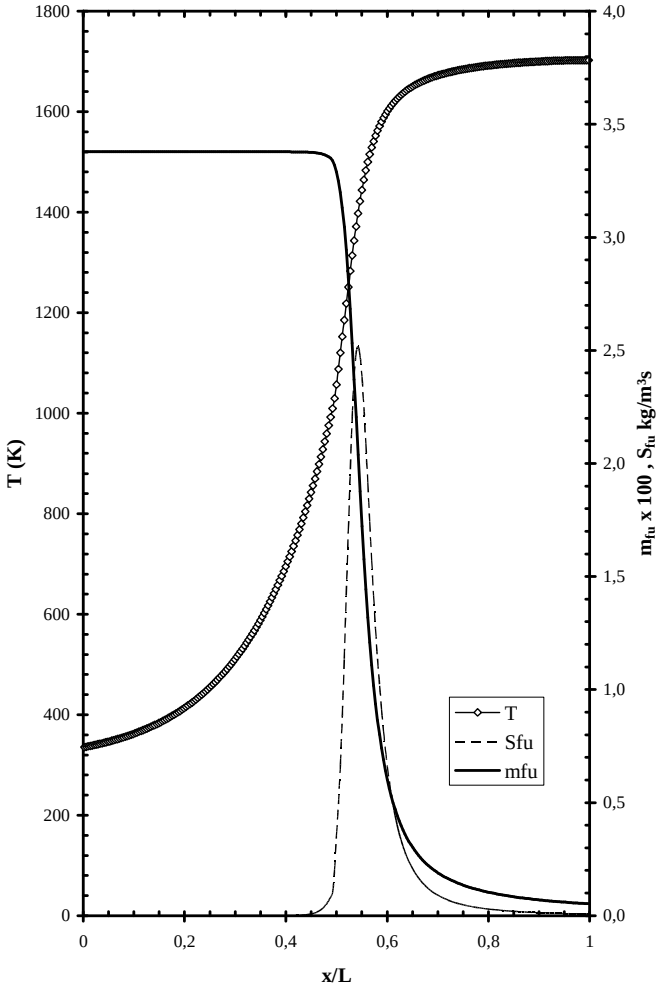

Figure 2.Axial temperature, mass fraction of fuel, and volumetric rate of fuel consumption profiles, y/H=0.5, Ψ=0.67.

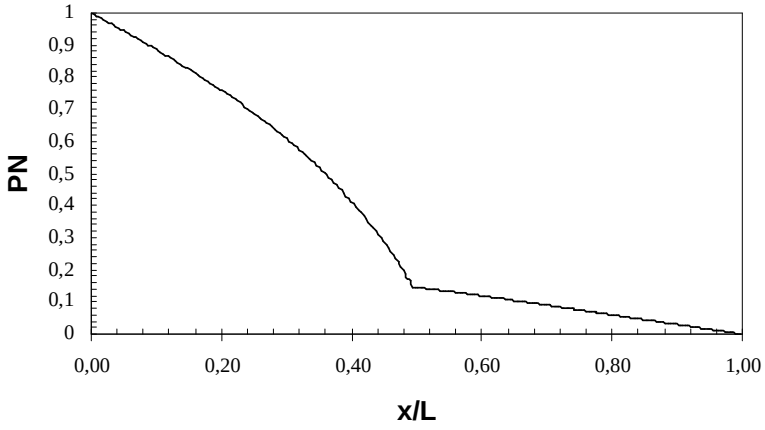

Figure 3. Pressure drop at the center line of the combustor, u_{in}=0.4 m/s.

4.4 Effect of inlet velocity on Temperature Profile

Figure 4 presents the effect of increase of inlet velocity on temperature profile for a rectangular adiabatic burner with an excess air ratio of 1.0. The figure indicates that, for laminar flows, the flame moves downstream, and stabilizes in an adiabatic temperature higher.

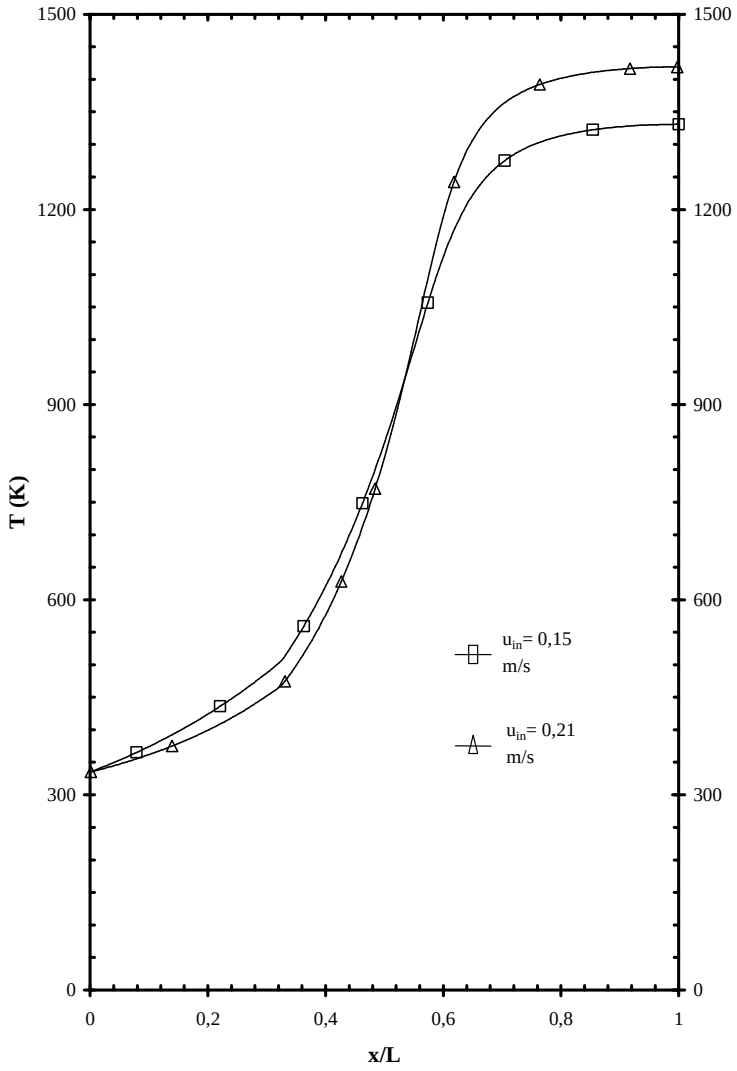

Figure 4. Temperature profiles for different inlet velocities, Ψ=1.0.

Note that decreasing the inlet velocity decreases the temperature, increasing the excess air ratio decreases the temperature also.

5. CONCLUSION

The model can be used to predict the fields of temperature, mass fraction of the fuel, pressure drop, velocity and the effect of the increase of the power in a two dimensional steady-state combustion problem within porous inert media. Further work will be carried out in order to simulate turbulent combustion in a porous medium with the macroscopic two-energy equation model.

6. ACKNOWLEDGEMENTS

The authors are thankful to CNPQ and FAPESP, Brazil, for their financial support during the preparation of this work.

7. REFERENCES

Yoshizawa, Y., Sasaki, K., and Echigo, R., 1988, "Analytical Study of the Structure of Radiation Controlled Flame," Int. J. Heat Mass Transf., 31, pp. 311–319. [Inspec] [ISI]

Hsu, P.-F., Howell, J. R., and Matthews, R. D., 1993, "A Numerical Investigation of Premixed Combustion Within Porous Inert Media," ASME J. of Heat Transfer, 115, pp. 744–750.

Baek, S. W., 1989, "The Premixed Flame in a Radiatively Active Porous Medium," Combust. Sci. Technol., 64, pp. 277–287.

Neef, M., Knaber, P., Summ, G., 1999, Numerical Bifurcation Analysis of Premixed Combustion in Porous Inert Media, unpublished, http://citeseer.csail.mit.edu/197085.html

Howell, J. R., Hall, M. J., and Ellzey, J. L., 1996, "Combustion of Hydrocarbon Fuels Within Porous Inert Media," Prog. Energy Combust. Sci., 22, pp. 121–145.

Trimis, D., and, Durst, F., 1996, Combustion in a Porous Medium Advances and Applications, Combust. Sci. Technol, Vol. 121, pp. 153-168.

Mohamad, A.A., Ramadhyani, S., Viskanta, R, 1994.Modeling of Combustion and Heat-Transfer in a Pcked-Bed with Embedded Coolant Tubes, *Int. J Heat and Mass Transfer*. vol. 37. (8) pp.1181-1191.

Pantangi, V. K. and S.C. Mishra, Combustion of gaseous hydrocarbon fuels within porous media – National Conference on Advances in Energy Research, 4-5 December 2006, IIT Bombay.

De Lemos. M. J. S. and Pedras. M. H. J.. 2001. Recent Mathematical Models for Turbulent Flow in Saturated Rigid Porous Media. *ASME Journal of Fluids Engineering*. vol. 123 (4). pp. 935-940.

De Lemos. M.J.S. Mesquita. M.S. Turbulent Mass Transport in Saturated Rigid Porous Media. *Int. Comm. In Heat & Mass Transfer*. 30 (1). pp. 105-113. 2003

Kaviany. M.. 1995. *Principles of Heat Transfer in Porous Media*. 2nd edn. Springer. New York.

Nakayama. A. and Kuwahara. F.. 1999. A Macroscopic Turbulence Model for Flow in a Porous Medium. *ASME Journal of Fluids Engineering*. vol. 121. pp. 427-433.

Patankar. S. V.. 1980. *Numerical Heat Transfer and Fluid Flow*. Hemisphere. New York.

Pedras. M. H. J. and de Lemos. M. J. S.. 2001a. Macroscopic Turbulence Modeling for Incompressible Flow Through Undeformable Porous Media. *Int. J. Heat Mass Transfer*. vol. 44 (6). pp. 1081-1093.

Pedras. M. H. J.. Rocamora. F. D. and de Lemos. M. J. S.. 2003. Simulation of Turbulent Thermal Dispersion in Porous Media Using a Periodic Cell with Prescribed Heat Flux at the Boundaries. *Proc. of 3rd Int. Conf.. Computational Heat and Mass Trans.*. May 26-30. Banff. Canada.

Pedras, M. H. J., and de Lemos, M. J. S., 2000, "On the Definition of Turbulent Kinetic Energy for Flow in Porous Media," Int. Commun. Heat Mass Transfer, 27_2_, pp. 211–220.

Pedras, M. H. J., and de Lemos, M. J. S., 2001a, "Macroscopic Turbulence Modeling for Incompressible Flow Through Undeformable Porous Media," Int. J. Heat Mass Transfer, 44_6_, pp. 1081–1093.

Pedras, M. H. J., and de Lemos, M. J. S., 2001b, "Simulation of Turbulent Flow in Porous Media Using a Spatially Periodic Array and a Low-Re Two-Equation Closure," Numer. Heat Transfer, Part A, 39_1_, pp. 35–59.

Pedras, M. H. J., and de Lemos, M. J. S., 2001c, "On the Mathematical Description and Simulation of Turbulent Flow in a Porous Medium Formed by an Array of Elliptic Rods," ASME J. Fluids Eng., 123_4_, pp. 941–947.

Lim, I- G., Matthews, R.D., 1993, Development of a Model for Turbulent Combustion Within Porous Inert Media Trensp. Phenm. Therm. Eng., Begell House Inc. Publ., pp 631-636

Jones, W.P., Launder, B.E., 1972, The Prediction of Laminarization with Two-Equation Model of Turbulence , Int. J. Heat & Mass Transfer, vol. 15, pp. 301 – 314,

Sahraoui, M., Kaviany, 1995, Direct simulation vs Time-Averaged Treatment of Adiabatic, Premixed Flame in a Porous Medium, Int. J. Heat Mass Transfer, v.18, pp. 2817-2834.

Pedras, M.H.J., de Lemos, M.J.S., "Computation of turbulent flow in porous media using a Low Reynolds $k-\varepsilon$ model and an infinite array of transversally-displaced elliptic rods", Numerical Heat Transfer Part A – Applications, 2003, 43 (6), 585 – 602.